Bulletin of Engineering Geology and the Environment (2019) 78:2345–2354
https://doi.org/10.1007/s10064-018-1307-5

ORIGINAL ARTICLE

Geotechnical properties and microstructure of lime-stabilized silt clay

Fu Zhu[1] · Zechuang Li[2] · Weizhi Dong[1] · Yangyun Ou[1]

Received: 11 February 2018 / Accepted: 10 May 2018 / Published online: 22 May 2018

Abstract

The geotechnical properties and microstructures of lime-stabilized silt clay from Jilin province, China, were studied in detail. Laboratory tests were conducted to evaluate the effects of lime content and curing time on the overall soil properties, including compaction characteristics, Atterberg limits, particle size distribution, pH, stress–strain behavior, peak strength, shear strength parameters, and California bearing ratio (CBR). The stabilized mechanisms of lime in silt clay were examined, and the observed test results were explained based on the results of scanning electron microscropy (SEM) and X-ray diffraction analyses of the specimens. Lime content and curing duration significantly influenced the geotechnical properties and microstructure of the lime-stabilized silt clay specimens. An increase in lime content resulted in increases in compaction water content, liquid limit, plastic limit, sand size-fractions, pH, peak strength, cohesion, internal friction angle, and the CBR, but led to a reduction in the plasticity index, silt fractions, clay fractions, swelling capacity, and water absorption. Also, the addition of lime to silt clay changed this soil type from a ductile to a brittle material. The optimum lime content of the silt clays from Jilin province was determined to be approximately 5–7%. SEM micrographs showed that a white cementitious gel was formed after the addition of lime and that peaks related to smectite, illite, kaolinite, and quartz appeared to be sharper after stabilization with lime and a 90-day period of curing. These results show that the geotechnical properties of lime-stabilized silt clay are affected by the microstructural organization of the silt clay itself.

Keywords Silt clay · Lime stabilization · Physical properties · Mechanical properties · Microstructure

Introduction

Jilin province in northeastern China was selected as the location for this study. Road subgrades and embankments in this province are subject to rain and successive freeze–thaw cycles which, together with inadequate compaction, significantly reduce the durability of the roads. If paved roads with low subgrade strength are constructed in these regions, thicker pavement is required; however, studies on the engineering properties of subgrade samples have revealed that it is desirable to improve the subgrade strength of the roads. There are several options open to engineers to improve the structural capacity of the pavements in areas of poor subgrades, including the use of soil stabilization materials such as cement, lime, fly ash, and gypsum (Lo and Wardani 2002; Hebib and Farrell 2003; Sariosseiri and Muhunthan 2009; Cuisinier et al. 2011; Rahardjo et al. 2013). The best soil stabilization material in a given setting depends on the cost, soil type, performance, and local experience.

Vast deposits of soils with poor engineering properties are widely distributed throughout rural and regional China. These soils pose significant challenges to road design and construction. One of these soil types is silt clay, which occurs in all of the cities of Jilin province (Zhan et al. 2015) and exhibits poor strength and stability. These soils can be the source of many engineering problems, such as large differential settlement, pavement cracking, and infrastructure instability, if there is no effective soil improvement (Puppala et al. 2004).

✉ Zechuang Li
lzc@nefu.edu.cn

Fu Zhu
zhufu_1981@163.com

[1] School of Transportation Science and Engineering, Jilin Jianzhu University, Changchun 130118, China

[2] School of Civil Engineering, Northeast Forestry University, Harbin 150040, China

Consequently, engineering projects aimed at improving the engineering properties of silt clay in a practical and cost-effective manner must be implemented.

Lime is a construction material that has been used by humans for more than 2000 years. However, the use of lime in geotechnical engineering was limited until 1945 (Herrin and Mitchell 1961). Today, soil stabilization with lime is a common technique in earthworks, including highways, embankments, dikes, airports, foundation bases, among others (Wilkinson et al. 2010). Lime is mainly used to dewater the soil in order to improve its workability and bearing capacity. Lime modification is widely used for building embankments and subgrades from clayey soil, since the effect is rapid and it modifies many of the geotechnical characteristics of the soil, including the plastic limit, shear strength, and soil compaction characteristics. The pozzolanic reaction between soil minerals and lime in the presence of water leads to the formation of secondary cementitious products, thereby increasing soil cohesion and resistance (Locat et al. 1990; Boardman et al. 2001; Runigo et al. 2011; Pomakhina et al. 2012). Boardman et al. (2001) showed that two distinct processes occur when lime is added to a wet soil: modification and stabilization. Many researchers attribute the improved geotechnical properties of lime-stabilized soil to four basic reactions: flocculation, cation exchange, lime carbonation, and the pozzolanic reaction (Eades and Grim 1960; Ingles and Metcalf 1972; National Lime Association 2004; Al-Rawas and Goosen 2006; Cuisinier et al. 2011).

This paper presents a comprehensive summary of investigations into the geotechnical properties and microstructural characteristics of lime-stabilized silt clay. A series of laboratory tests were performed to study the effect of lime content and curing time on Atterberg limits, compaction characteristics, particle size distribution, pH value, stress–strain characteristics, peak strength, shear strength, California bearing ratio (CBR), swelling capacity, and water absorption. Scanning electron microscopy (SEM) and X-ray diffraction (XRD) analyses were also performed to further investigate changes in the microstructural characteristics and clay minerals. Based on these results, we discuss the evolution of mechanical properties of stabilized silt clay during the curing period and draw links between the microstructural characteristics and basic engineering properties, and we clarify the potential of lime as a stabilizer to improve the engineering properties of silt clay.

Materials and methods

Raw materials

In this study, silt clay, lime, and water were combined to make compacted mixtures of silt clay and lime. Silt clay is a typical soil material in Jilin province and does not meet the requirements for highway subgrade construction in cold regions. According to the Technical Specification for Construction of Highway Subgrade in China, silt clay should be improved or removed during highway construction. The basic properties of soil samples collected for this study are presented in Tables 1 and 2. The XRD analyses showed that the composition of the soil under study was 54% primary mineral, including quartz, alkali feldspar, plagioclase, and 46% secondary minerals, including an illite/smectite (I/S) mixed layer, illite, and kaolinite; the clay mineral fraction was predominantly (34%) composed of an I/S mixed layer.

Table 1 Physicochemical properties of silt clay samples

Property	Characteristic
Specific gravity	2.694
Grain size distribution	
Clay < 0.005 mm (%)	41.81
Silt 0.005–0.075 mm (%)	55.25
Sand (0.075–2 mm) (%)	2.94
Liquid limit (%)	32.4
Plasticity limit (%)	19.5
Plasticity index	12.9
Optimum moisture content (%)	13.8
Maximum dry unit weight (g/cm^3)	1.898
pH value	8.96

The lime used in this study, supplied by the Shuangyang Company of Jilin province, is a very fine lime that can pass through a 2-mm sieve. The chemical composition of the tested this lime is shown in Table 2.

Sample preparation

The natural silt clay collected was air dried and broken down to particle sizes that could pass a 2-mm sieve for unconsolidated, undrained triaxial compression tests and pH tests, and through a 5-mm sieve for the CBR tests. The amounts of lime and water added were calculated as percentages of the dry weight of the soil sample; the amounts tested were 0, 3, 5, 7, 9, and 11%, respectively. The lime was first mixed with an additional amount of water to achieve the optimum moisture content (OMC) and then mixed thoroughly to achieve homogeneity before being was poured into a steel mold (triaxial compression test: inner diameter 39.1 mm, height 80 mm; CBR test: or inner diameter 152 mm, height 170 mm) and compacted to the maximum dry density (MDD). All specimens were prepared using the static compaction method specified in the GB/T 50123-1999 Standard of the China National Standards for geotechnical tests in China. The values of OMC and MDD for stabilized silt clay with different lime contents from the standard Proctor compaction method specified in the GB/T50123-1999 Standard are shown in Fig. 1. The

Table 2 Oxide chemistry of silt clay and lime samples

Oxide chemistry	Silt clay characteristic (%)	Lime characteristic (%)
Silicon oxide (SiO_2)	67.17	2.13
Aluminum oxide (Al_2O_3)	14.99	0.32
Ferric oxide (Fe_2O_3)	4.95	0.23
Calcium oxide (CaO)	1.29	71.58
Magnesium oxide (MgO)	1.30	0.38
Potassium oxide (K_2O)	3.33	0.07
Sodium oxide (Na_2O)	1.90	0.04
Titanium dioxide (TiO_2)	0.79	0.02
Phosphorus oxide (P_2O_5)	0.08	0.04
Manganese oxide (MnO)	0.09	0.01
Others	3.87	24.97
Total	99.76	99.78

specimens (diameter 39.1 mm, height 80 mm) were extruded from the molds using a hydraulic jack, and the compacted samples were sealed in plastic wrap to minimize moisture loss and placed in a room with controlled temperature (20 °C) and relative humidity for curing. The triaxial compression and CBR tests were conducted after 7 days of curing. Soil samples (approximately 1 cm^3) were retrieved from carefully hand-broken identical specimens after 7 and 90 days of curing for SEM analysis. The freeze-drying technique was used to dehydrate soil specimens for the SEM tests, as suggested by Cuisinier et al. (2011) and Li and Zhang (2009). Liquid nitrogen with a boiling point of − 195° was used to quick-freeze the specimens, following which the specimens were placed in a vacuum chamber at − 50 °C for 24 h and then dried by sublimation of the frozen water.

Testing methods

Prior to this investigation, the engineering properties of the silt clay under study, including specific gravity, consistency limit, grain size distribution, and pH, were determined in the laboratory according to the relevant tests specified in the GB/T 50123-1999 Standard.

To determine the OMC and MDD, mixtures with a lime content of 0, 3, 5, 7, 9, or 11% were produced by mixing the soil for 12 h after the addition of lime and water. A series of standard Proctor compaction tests were then carried out according to the relevant specifications in the GB/T 50123-1999 Standard to determine the OMC and MDD of all mixtures.

For the particle size analysis test, mixtures with a lime content of 0, 3, 5, 7, 9, or 11% were produced by mixing the soil for 7 days after the addition of lime and water. These lime-stabilized specimens were used for the particle size analysis test after first being broken down to a particle size that could pass through a 0.15-mm sieve. The samples were prepared according to the relevant specifications for Atterberg limits.

To characterize the strength of lime-stabilized silt clay, we performed unconsolidated undrained triaxial compression tests in accordance with the specification of the GB/T 50123-1999 Standard by fixing the strain rate at 0.8% per minute under a confining pressure (σ_3) of 30, 100, or 150 kPa. A certain quantity of the stabilized silt clay was immediately sampled from the broken unconsolidated undrained triaxial compression specimens to determine the pH value. Specifically, 10 g of the sieved soil sample and 50 mL of deionized water were mixed thoroughly in a beaker and left to stand for 1 h; the pH values of the specimens were then measured by placing the pH probe of a basic benchtop pH meter (model pHS-25; BiocoTek, Beilun, Ningbo, China) into the supernatant.

CBR values are commonly used in mechanistic design and as indicators of the strength and bearing capacity of subgrade soil and subbase and base course material for use in road construction. The CBR of a soil is the ratio obtained by dividing the stress required to cause a standard piston to penetrate 2.5 and 5.0 mm into the soil by a standard penetration stress at each depth of penetration (GB/T 50123-1999 Standard). The CBR may be thought of as an index value that compares the strength of the soil to that of crushed rock. In our study, we conducted CBR tests for soaked conditions. To obtain this condition, the sample with mold was placed in water baths in a controlled temperature environment and soaked for 96 h to achieve full (or nearly full) saturation. A surcharge stress of 3.5 kPa was applied to the sample using steel weights. Initial and final vertical deflection readings were taken using a tripod with a dial gauge which enabled the swelling capacity to be calculated as a percentage of the initial height of the sample. The sample with mold was then removed from the water bath, and excess water was absorbed with filter paper; after standing for 15 min, the steel weights, porous roof, porous bottom plate, and filter paper were removed. Water absorption was calculated by weighing the sample mass. Following the 96-h soaking period, CBR tests were performed by fixing the

penetration rate at 1 mm per minute, and the CBR performance of each sample was evaluated at penetrations of 2.5 and 5.0 mm. The CBR values reported here are average values of two similar samples.

A comparative SEM study to observe sample morphology was conducted using samples of unmodified silt clay and 7% lime-stabilized silt clay and a Hitachi scanning electron microscope (model TM3030; Hitachi Ltd., Tokyo, Japan). Prior to the SEM analysis, the sample was coated with 100-Å thin layer of gold and palladium for 38 s using a Poloran E5100 sputter coater (Quorum Technologies, Lewes, UK) under a vacuum of 10^{-3} Torr.

XRD analysis was conducted on broken specimen that had been air-dried, ground, and passed through a sieve (diameter < 0.075 mm), The X-ray diffractometer (model D-2700; Yaoyuan, Dandong, China) was equipped with a Cu-Kα (λ = 1.5148 Å) X-ray tube with an input voltage of 35 kV and a current of 25 mA. Specimens were scanned for two-theta values ranging between 5° and 60°, with a step length of 0.02° and a scanning rate of 1° per minute.

Results and analysis

Compaction characteristics

The relationship between the dry density and moisture content of compacted silt clay and lime mixtures with different lime contents is shown in Fig. 1. It should be noted that the MDD values of the silt clay are much higher than those obtained for the lime-treated silt clay. All MDD values can be seen to fall in the range of 1.90 to 1.75 g/cm^3, while the OMC values range from 13.8 to 15.9%. With increasing lime content, the compaction curve moves downward and toward the right, indicating that with increasing lime content, the MDD value decreases and the OMC value increases. This behavior can be attributed to the tendency of lime to absorb water in order to complete its hydration, thereby increasing the OMC. Further, the immediate reactions represented by flocculation and agglomeration tend to increase the OMC and decrease the MDD values, respectively (Aldaood et al. 2014). The compaction curve of lime-stabilized silt clay is less steep than that of unmodified silt clay. In general, the compaction curve becomes flatter with increasing lime content. The range of compaction water content is wider than that of silt clay in construction.

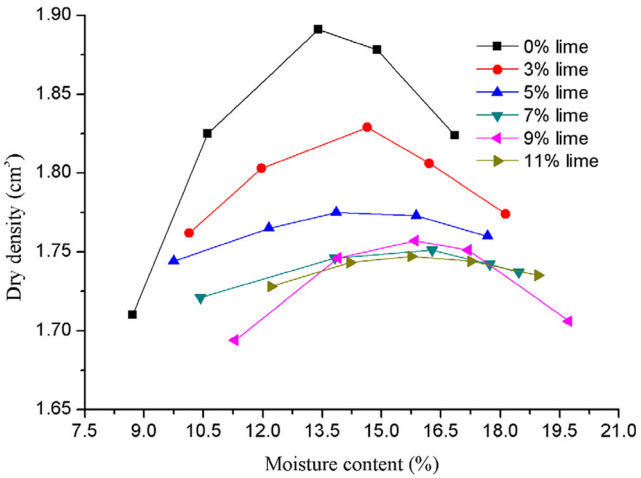

Fig. 1 Compaction curves of stabilized silt clay with different lime content

Atterberg limits

The effect of lime content on the liquid limit, plastic limit, and plasticity index is shown in Fig. 2. Both the liquid limit and plastic limit can be seen to increase with increasing lime content, whereas the plasticity index decreases with increasing lime content. This result is consistent with data on wood ash-stabilized or lime-stabilized soils reported in the literature (Locat et al. 1990).

The higher liquid limit and plastic limit of the stabilized silt clay reflects the presence of water trapped within the intra-aggregate pores, which significantly increases the Atterberg limits of the low-plasticity silt clay. In lime-stabilized soils, cation exchange, pozzolanic reactions, and the formation of calcium silicate hydrate significantly affect the Atterberg limits of the soils.

Particle size analysis

The effect of lime content on the settling rate, which increases with increasing lime content, is shown Fig. 3. It can be seen that the greater the lime content, the faster the suspension turbidity is reduced, indicating that the incorporation of lime

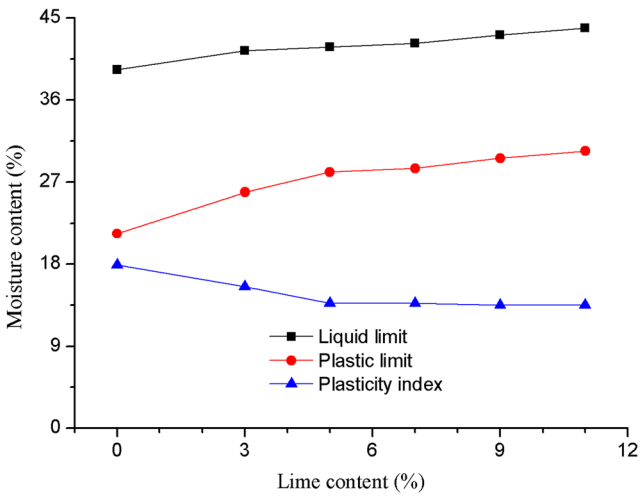

Fig. 2 Effect of lime content on Atterberg limits of stabilized silt clay

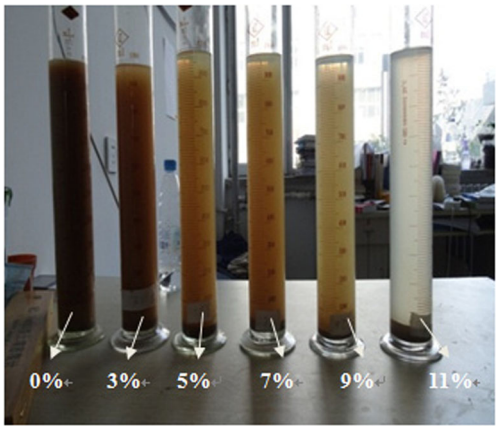

Fig. 3 Effect of lime content on settling rate

significantly increases the mean particle size of the smaller particles in suspension.

With increasing lime content, the sand fractions increased while the silt and clay fractions decreased. This shift in the distribution of particle size to the coarser fraction suggests that the addition of lime causes chemical reactions leading to the flocculation of clay particles. These results are compatible with the findings of Sharma et al. (2012), who found that with increasing lime content, there was an apparent reduction in clay content and a corresponding increase in the percentage of coarse particles.

Alkalinity of lime stabilized silt clay

The measured pH values of the silt clay and stabilized specimens treated with different amounts added lime during their curing times are shown in Fig. 4. The pH values of all the specimens can be seen to decrease with curing time, regardless of the lime content. The pH values do increase rapidly with lime content, approaching equilibrium with further increases in lime content, due to the increased concentration of hydroxyl

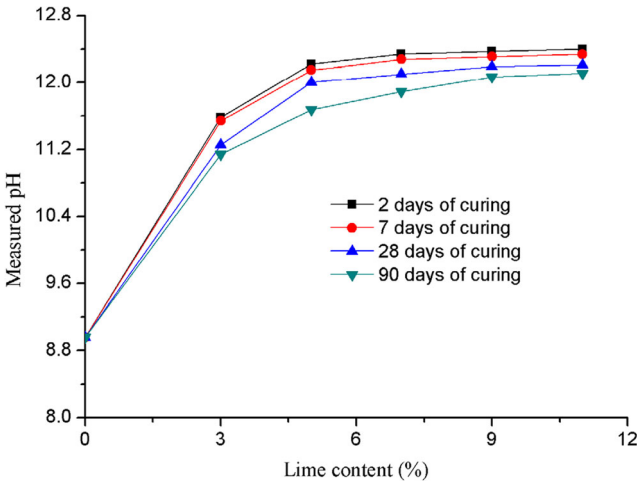

Fig. 4 Measured pH values for lime-stabilized silt clay with different curing times

ions (OH^-) in pore water induced by the addition of lime. Although the pH values of all specimens increase with lime content, no pH value exceeds 12.4.

Table 3 shows the particle size distribution for silt clay and lime-stabilized silt clay, as obtained from the sieve and hydrometer analyses. Particle size distributions were altered by the addition of the lime.

Stress–strain behavior and peak strength

The typical stress–strain curves for silt clay and lime-stabilized specimens after 7 days of curing are given in Fig. 5. The natural silt clay exhibits ductile characteristics, exhibiting a gradual drop in the post-peak stress with increasing strain (Fig. 5a). Following the addition of lime, the stabilized soil behaves like a brittle material (Fig. 5b), exhibiting a rapid drop in the post-peak stress with increased strain. Figure 5 also shows that the strain at failure for untreated silt clay is dramatically larger than that of the stabilized specimens, indicating that the addition of lime changes the response of silt clay from that of a ductile material to one of a brittle material.

The peak strength of specimens increased both dramatically and rapidly with increasing lime content and increasing confining pressure, as shown in Fig. 6, approaching equilibrium at approximately 7% lime content. This result suggests that the optimum lime content should not be higher than 7%.

Under the condition of a confining pressure of 30 kPa, the peak strength of lime-stabilized silt clay samples with 3, 5, 7, 9, and 11% lime content refers to peak strength that is 1.74-, 2.02-, 2.14-, 2.06-, and 2.11-fold higher, respectively, than that of silt clay. Under the condition of a confining pressure of 100 kPa, the peak strength of lime-stabilized silt clay samples with 3, 5, 7, 9, and 11% lime content refers to a peak strength that is 1.98-, 2.29-, 2.86-, 2.59-, and 2.60-fold higher, respectively, than that of silt clay. Under the condition of a confining pressure of 150 kPa, the peak strength of lime-stabilized silt clay samples with 3, 5, 7, 9, and 11% lime content refers to a peak strength that is 2.15-, 2.51-, 2.81-, 2.49-, and 2.58-fold higher, respectively, than that of silt clay.

Variation of shear strength parameters

The values of cohesion and internal friction angle tested after 7 days of curing are shown in Fig. 7. Both cohesion and the internal friction angle of lime-stabilized specimens can be seen to increase with lime content. The added amounts of lime also appear to have a significant influence on the development of cohesion (Fig. 7a).

Figure 7b shows that the internal friction angle increases initially and then decreases slightly as lime content increases from 3 to 11%. The maximum internal friction angle of 11.3° is observed at a lime content of 7%, which is 3.4-fold higher than that of the untreated specimen. The results of the triaxial

Table 3 Particle size distributions analysis results for unmodified and lime-amended soils

Lime content (%)	Particle size fraction (%)		
	> 0.075 mm (sand)	0.005-0.075 mm (silt)	< 0.005 mm (clay)
0	2.94	55.25	41.81
3	18.04	50.79	31.17
5	39.39	48.14	12.48
7	43.23	44.14	12.63
9	46.55	42.22	11.23
11	39.46	49.92	10.62

compression tests suggest that the optimum lime requirement for strength improvement could be close to 7%.

The cohesion of lime-stabilized silt clay with 3, 5, 7, 9, and 11% lime content refers to a cohesion that is 1.63-, 1.95-, 2.01-, 2.14-, and 2.48-fold higher, respectively, than that of silt clay. The internal friction angle of lime-stabilized silt clay with 3, 5, 7, 9, and 11 lime content refers to an internal friction angle that is 2.32-, 2.87-, 3.33-, 3.05-, and 2.52-fold higher, respectively, than that of silt clay.

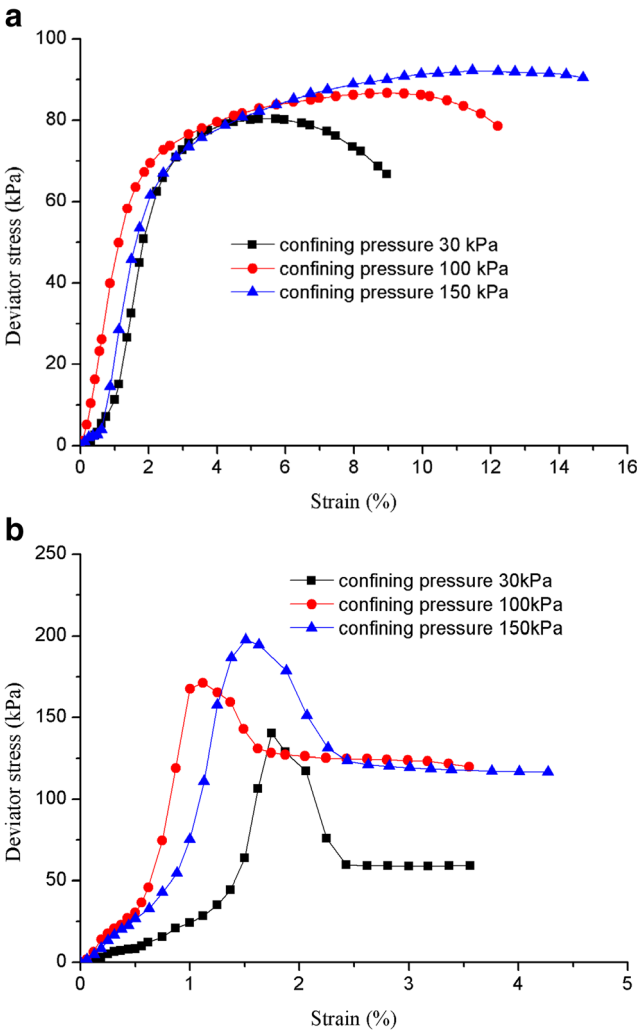

Fig. 5 Stress–stain curves of silt clay (**a**) and lime-stabilized (**b**) specimens after 7 days of curing

California bearing ratio

The variation in the CBR in lime-stabilized silt clay is shown in Fig. 8. The change in the CBR with increasing lime concentration appears to be generally similar to that seen in peak strength (Fig. 6). The CBR initially increases with increasing lime content, but approaches equilibrium at lime contents of > 5%. This result is consistent with the results of the triaxial compression tests discussed in the section Variation of shear strength parameters and indicates that lime-stabilized silt clay shows potential as a subgrade or pavement construction material.

Swelling capacity and water absorption

As shown in Fig. 9, both swelling capacity and water absorption decrease with increasing lime content up approximately 3–5% lime content, above which no additional beneficial changes were observed. When the lime content is increased to 3%, the swelling capacity suddenly decreases by 4.24%, but subsequent decreases are smaller (Fig. 9a). In contrast, the

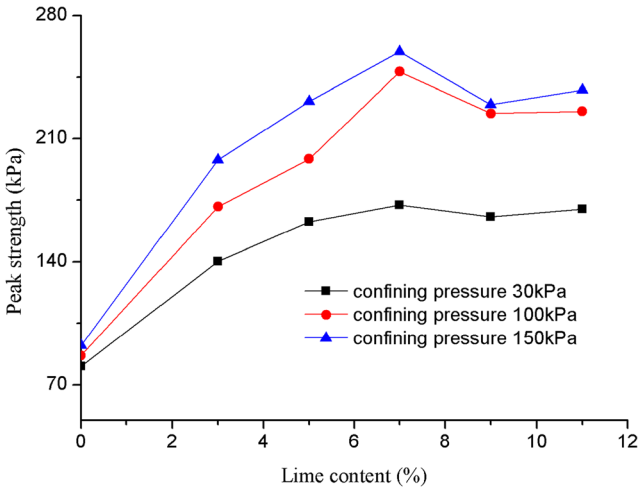

Fig. 6 Variation in peak strength in lime-stabilized silt clay

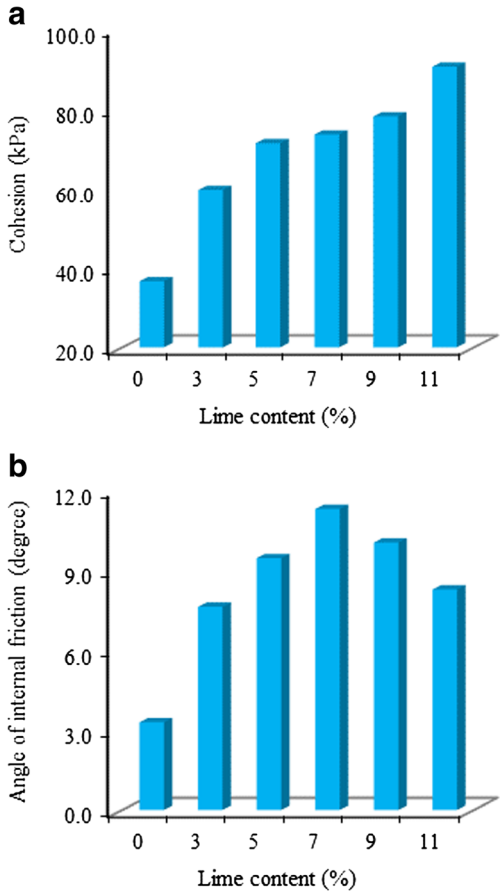

Fig. 7 Variation in cohesion (**a**) and internal friction angle (**b**) in lime-stabilized silt clay

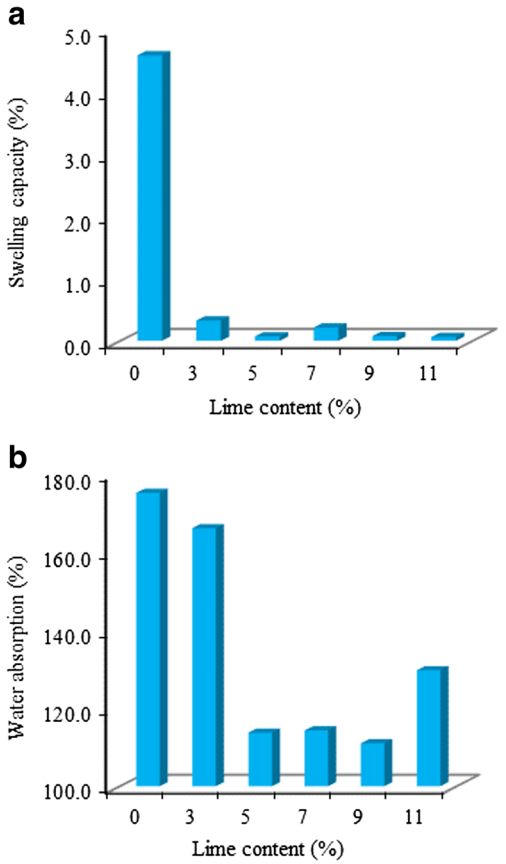

Fig. 9 Variations in the swelling capacity (**a**) and water absorption (**b**) in lime-stabilized silt clay

swelling capacity of lime-stabilized silt clay is observed to be the lowest at 5% lime content, increasing slightly when the lime content exceeds 5%. Figure 9b shows that the water absorption decreases initially and then increases slightly as the lime content increases from 3 to 11%, consistent with the results of the swelling capacity test. With increases in the lime content from 0 to 9%, water absorption decreased by 64 g.

This phenomenon reflects the fact that as the cementitious products of lime-soil chemical reactions increase with increased immersion time, the microstructure of the soil is changed, and some of the pores become filled with the cementitious material, thereby increasing the soil density. The pore volume of the water that can be accommodated when the sample is immersed is reduced, resulting in a decrease in water absorption. However, when the lime content exceeds 9%, the content of free lime is excessive, and the soil density decreases due to the excess lime, which leads to an increase in water absorption.

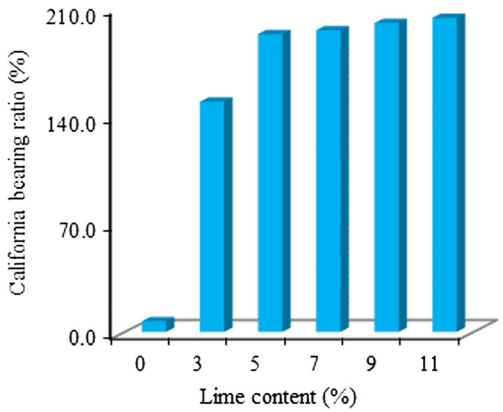

Fig. 8 Variations in the California bearing ratio in lime-stabilized silt clay

SEM analysis

The microstructures of the silt clay with lime contents of 0 and 7% after 7 and 90 days of curing at a magnification of 5000× are shown in Fig. 10. SEM images of silt clay (Fig. 10a) and 7% lime-stabilized silt clay (Fig. 10b, c) show very different microtextures. The lime treatment can be seen to have strongly modified the original silt clay texture at the micrometer scale.

Figure 10a, b show that the flat and large particles in the silt clay sample are highly divided, leading to many packets of particles and forming a less compact structure than that observed in the stabilized sample. Figure 10b shows that in the lime-stabilized silt clay, white cementitious gel and $Ca(OH)_2$ have formed in the pore spaces between aggregated soil

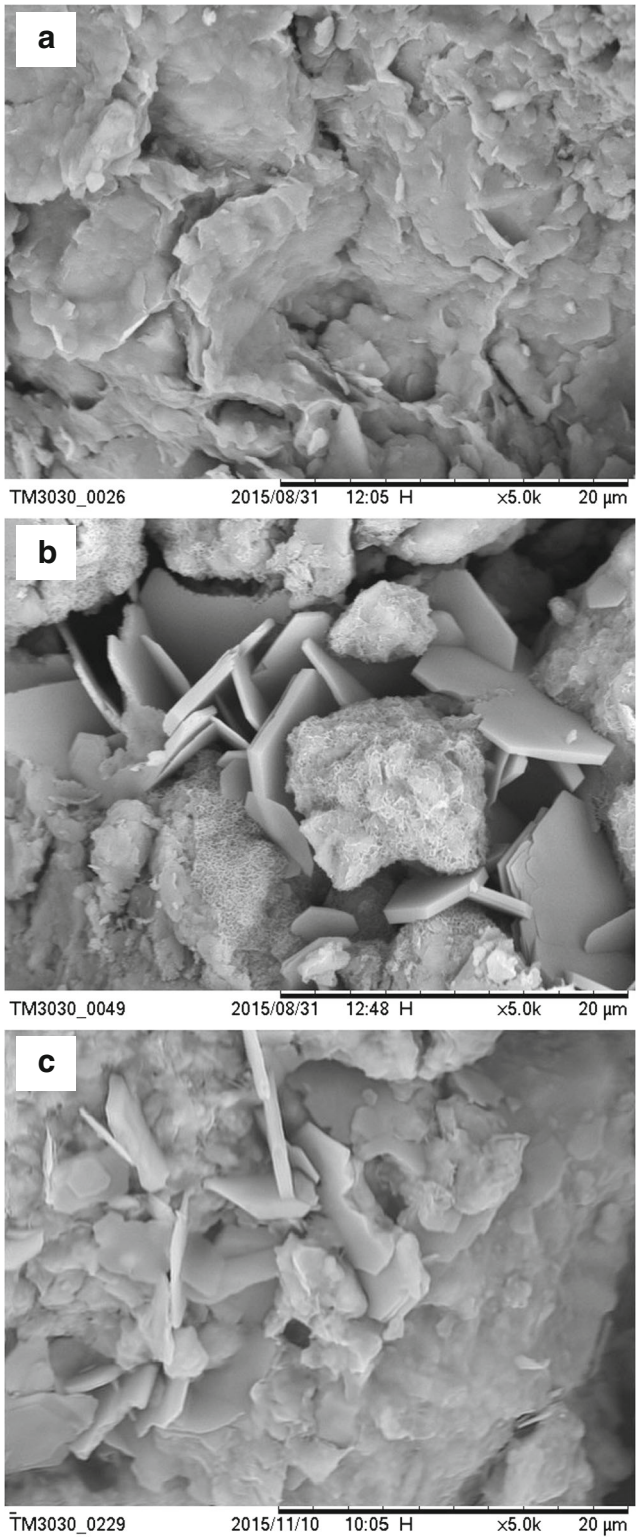

Fig. 10 Scanning electron microscopy images of silt clay (**a**), 7% lime-stabilized silt clay after 7 days of curing (**b**), and 7% lime-stabilized silt clay after 90 days of curing (**c**)

particles. One possible explanation is that when lime is initially admixed with dried clayey soil, it causes the clay particles to adopt hydrophobic behavior so that they are unable to form large aggregations when water is later added to the lime–silt clay mixture. Liu (2003) referred to this phenomenon as 'sandification'. Furthermore, the filling of pores between particles with white cementitious gel results in a decrease of the plasticity index and an increase in compressive strength.

A micrograph of soil stabilized with 7% lime content after a longer curing time of 90 days is shown in Fig. 10c. This image shows the binding and coating of aggregated soil particles, forming a densely packed and compacted structure, whereas relatively fewer white patches are observed. This relative absence of white patches reflects the consumption of cementitious gel in filling voids and binding particles, leading to a significant increase in strength (Mathew and Narasimha 1997; Nalbantoglu and Gucbilmez 2001).

XRD analysis

The mineralogical alteration and formation of new reaction compounds in silt clay with the addition of lime were examined by XRD analyses, as shown in Fig. 11. Figure 11, top shows the diffractogram for silt clay and reveals that the silt clay is composed of illite, smectite, kaolinite, and quartz. Figure 11, bottom shows that there are no significant peaks of cementitious compounds related to amorphous or non-crystalline compounds in the sample with 7% lime after a 90-day curing period. Similar characteristics were reported for other lime-stabilized soils by Jha and Sivapullaiah (2015). This results again confirms experimental results indicating that most of the lime is consumed to alter the physical soil properties through short-term processes such as flocculation and cation exchange, resulting in weak bonding between the soil particles and significant strength. However, peaks related to illite, smectite, and quartz do appear to be sharper in Fig. 11, bottom, confirming the alteration in structure.

Conclusions

The effects of lime on Atterberg limits, particle size distribution, peak strength, shear strength parameters, failure characteristics, CBR, swelling capacity, and water absorption of silt clay have been studied. Experimental results show that the addition of lime causes beneficial changes in the above-mentioned engineering properties of the silt clay tested in this investigation.

The addition of lime to silt lay soils results in an increase in the liquid limit and plastic limit, while the plasticity index decreases with increasing lime content. The reason for the higher liquid limit and plastic limit in stabilized silt clay is the presence of a certain quantity of water trapped within the intra-aggregate pores, which significantly increases the Atterberg limits of the low-plasticity silt clay. An increased

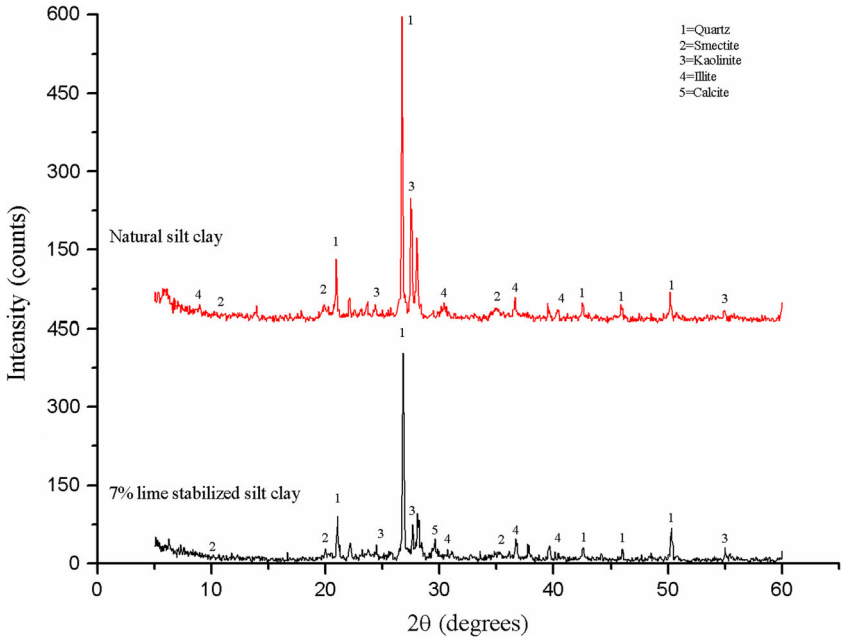

Fig. 11 X-ray diffraction analysis of silt clay (**top**) and 7% lime-stabilized silt clay (**bottom**) after 90 days of curing

particle settling rate also results from increasing lime content. Particle size distributions are shifted significantly to the coarser side as the lime percentage increases, possibly due to chemical reactions which cause the agglomeration of clay particles and an increase in the fraction of sand-size particles.

These engineering properties of lime-stabilized silt clay vary with and depend upon lime content. The peak strength, cohesion, and CBR increase with increasing lime content. An increase in lime content also contributes to an initial increase, followed by a slight decrease, in the friction angle of stabilized silt clay. The optimum gain in strength appears to be obtained with the addition of 5–7% lime.

Compared with silt clay, the optimum water content of lime-stabilized silt clay with 5 and 7% lime content is increased by 4.3 and 12.3% respectively; the liquid limit is increased by 6.4 and 7.4%, respectively; the plastic limit is increased by 6.7 and 7.1%, respectively; peak strength is increased by 102.4 and 114.3%, respectively; cohesion is increased by 150.2 and 101.3%, respectively; internal friction angle is increased by 6.14° and 7.99°, respectively; CBR is increased by 26.9- and 27.3-fold, respectively.

The increase in the lime content leads to a decrease in swelling capacity and water absorption, indicating that the addition of lime improves the engineering properties of silt clay through cation exchange, flocculation, and cementing. However, water absorption increases only slightly when the lime content exceeds 9%.

Samples of lime-amended silt clay were analyzed by SEM and XRD. The formation of white cementitious gel due to reactions between lime and silt clay was observed on the SEM micrographs. These reaction products bind the soil particles and increase soil strength. The XRD analyses show no new peaks at the shorter curing period due to amorphous or non-crystalline compounds in the lime-stabilized silt clay. Peaks of the principal component minerals are reduced after stabilization. Soil particles are coated and bonded with precipitated cementing material, and a more stable soil structure is formed after stabilization.

The engineering properties of lime-stabilized silt clay can be explained by changes in the fabric, cation exchange, and binding of soil particles by the cementitious compounds formed. The reduction in the plasticity of soil with lime is predominantly due to cation exchange, whereas the effect of flocculation is relatively less. However, the decrease in the dry density and the increase in the optimum water content and sand fractions are due to the flocculation and aggregation of the soil particles. The increase in the strength of lime-stabilized silt clay is due to the binding and coating of aggregated soil particles, with the formation of a densely packed and compacted structure that reflects the consumption of cementitious gel in filling voids and binding particles.

Acknowledgements This research is financially supported by the project of Education Department of Jilin Province (JJKH20170260KJ), the Project of Ministry of Housing and Urban-Rural Development (2017-K4-004), and the Plan Projects of Transportation Science and Technology in Jilin Province of China (2011103).

Compliance with ethical standards

Conflict of interests The authors declare that there are no conflicts of interest regarding the publication of this paper.

References

Aldaood A, Bouasker M, Al-Mukhtar M (2014) Geotechnical properties of lime-treated gypseous soils. Appl Clay Sci 88–89(3):39–48

Al-Rawas AA, Goosen MFA (2006) Expansive soils: recent advances in characterization and treatment. Taylor & Francis group/Balkema, London

Boardman DI, Glendinning S, Rogers CDF (2001) Development of stabilisation and solidification in lime-clay mixes. Geotechnique 51(6):533–544

Cuisinier O, Auriol JC, Borgne TL et al (2011) Microstructure and hydraulic conductivity of a compacted lime-treated soil. Eng Geol 123(3):187–193

Eades JL, Grim RE (1960) Reaction of hydrated lime with pure clay minerals in soil stabilization. Highw Res Board Bull 262:51–63

Hebib S, Farrell ER (2003) Some experiences on the stabilization of Irish peats. Can Geotech J 40(1):107–120

Herrin M, Mitchell H (1961) "Lime–soil mixtures." Bulletin No. 304. Highway Research Board, Washington DC

Ingles OG, Metcalf JB (1972) Soil stabilization: principles and practice. Butterworths, Sidney

Jha AK, Sivapullaiah PV (2015) Mechanism of improvement in the strength and volume change behavior of lime stabilized soil. Eng Geol 198(2):53–64

Li X, Zhang LM (2009) Characterization of dual-structure pore-size distribution of soil. Can Geotech J 46(46):129–141

Liu P (2003) Test and study into strengthening technique of overwet and high liquid limit soil subbase. Munic Eng Technol 21(2):97–102

Lo SR, Wardani SP (2002) Strength and dilatancy of a silt stabilized by a cement and fly ash mi. Can Geotech J 39(1):77–89

Locat J, Bérubé MA, Choquette M (1990) Laboratory investigations on the lime stabilization of sensitive clays. Can Geotech J 27(3):294–304

Mathew PK, Rao SN (1997) Effect of lime on cation exchange capacity of marine clay. J Geotech Geoenviron Eng 123(2):183–185

Nalbantoglu Z, Gucbilmez E (2001) Improvement of calcareous expansive soils in semi-arid environments. J Arid Environ 47(4):453–463

National Lime Association (NLA) (2004) Lime-treated soil construction manual lime stabilization & lime modification. Technical brief. National Lime Association, Arlington

Pomakhina E, Deneele D, Gaillot AC et al (2012) 29 Si solid state NMR investigation of pozzolanic reaction occurring in lime-treated ca-bentonite. Cem Concr Res 42(4):626–632

Puppala AJ, Griffin JA, Hoyos LR et al (2004) Studies on sulfate-resistant cement stabilization methods to address sulfate-induced soil heave. J Geotech Geoenviron Eng 130(4):391–402

Rahardjo H, Santoso VA, Leong EC et al (2013) Use of recycled crushed concrete and Secudrain in capillary barriers for slope stabilization. Can Geotech J 50(6):662–673

Runigo BL, Ferber V, Cui YJ et al (2011) Performance of lime-treated silty soil under long-term hydraulic conditions. Eng Geol 118(1–2): 20–28

Sariosseiri F, Muhunthan B (2009) Effect of cement treatment on geotechnical properties of some Washington state soils. Eng Geol 104(1):119–125

Sharma NK, Swain SK, Sahoo UC (2012) Stabilization of a clayey soil with fly ash and lime: a micro level investigation. Geotech Geol Eng 30(5):1197–1205

Wilkinson A, Haque A, Kodikara J, Adamson J, Christie D (2010) Improvement of problematic soils by lime slurry pressure injection: case study. J Geotech Geoenviron Eng 136(10):1459–1468

Zhan GF, Zhang Q, Fu Z et al (2015) Research on influence of freeze-thaw cycles on static strength of lime-treated silty clay. Rock Soil Mech 36:351–356